

## Analysis of electromechanical behaviour of $(1-x)\text{PMN}-x\text{PT}$ (with $x \leq 0.1$ ) bulk ceramics

Martine Lejeune<sup>a,\*</sup>, Edith Lattard<sup>a</sup>, Sylvie Kurutcharry<sup>a</sup>, Maksoud Oudjedi<sup>a</sup>,  
Dominique Imhoff<sup>b</sup>, René Guinebretiere<sup>a</sup>, Catherine Elissalde<sup>c</sup>, Pierre Abelard<sup>a</sup>

<sup>a</sup>S.P.C.T.S. UMR 6638, (E.N.S.C.I) Ecole Nationale Supérieure de Ceramique Industrielle, 47à 73 Av Albert Thomas, 87065, Limoges Cedex, France

<sup>b</sup>L.P.S, URA 0002, University of Paris-Sud Orsay, France

<sup>c</sup>ICMCB, University of Bordeaux I, Pessac, France

Received 30 July 1999; received in revised form 9 September 1999; accepted 26 October 1999

### Abstract

The electromechanical behaviour of the  $(1-x)\text{PMN}-x\text{PT}$  ( $x \leq 0.1$ ) bulk ceramics is studied in particular through the sensitivity of its nanostructure to the electric field, stress and temperature. At first, it was shown by deviation to the Curie–Weiss type behaviour that a local polarisation appears at a  $T_d$  temperature (around 200°C) i.e. largely above the temperature of the maximum of permittivity ( $T_m$ , respectively  $-13^\circ\text{C}$  and  $+36^\circ\text{C}$  for  $x = 0$  and 0.1), which is consistent with the nucleation of polar clusters within a paraelectric matrix. Moreover, the dielectric relaxation observed for  $0.9\text{PbMg}_{1/3}\text{Nb}_{2/3}\text{O}_3-0.1\text{PbTiO}_3-0.12\text{MgO}$ , in a large frequency range (100 Hz–15 MHz), and corresponding to a multi-Debye process with broadening of the relaxation time distribution as the temperature decreases, has been correlated to a nucleation and growth mechanism of polar clusters with decreasing temperature below  $T_d$ , which might result from the successive transitions of different compositions. This hypothesis has been confirmed by nanoanalysis thanks to EDXS and EELS techniques: in fact large fluctuations of the local composition around the nominal one have been revealed, lead and magnesium deficient areas enriched in niobium coexisting with nanodomains (around 10 nm) strongly enriched in lead and slightly in magnesium. Consequently, due to such heterogeneities, the material remains mainly paraelectric up to very low temperatures. This effect can be balanced by the application of a high electric field which induces the growth of the polar clusters up to a macroscopic ferroelectric transition for some conditions of temperature and electric field. The specific electromechanical characteristics of  $0.9\text{PMN}-0.1\text{PT}$  are reported, in particular the strong dependence of their elastic compliance with the electric field, the prestress applied to the material and the temperature. This behaviour is attributed to the growth of compliant polar clusters induced by decreasing temperature or increasing electric field and inhibited by the application of a uniaxial stress. Finally, as  $0.9\text{PMN}-0.1\text{PT}$  bulk ceramics are characterised by a tunable compliance, their potential interest as active vibration control is presented and its electromechanical behaviour as actuator, under a sinusoidal electrical signal added to a 0.6 kV/mm DC electric field, is characterised. © 2000 Elsevier Science Ltd and Techna S.r.l. All rights reserved.

**Keywords:** Electromechanical behaviour

### 1. Introduction

Lead based magnesium niobate materials have been largely studied for the last 10 years to develop electrostrictive actuators for commercial applications requiring large field induced-strains associated to low hysteresis [1]. Indeed,  $(1-x)\text{PbMg}_{1/3}\text{Nb}_{2/3}\text{O}_3-x\text{PbTiO}_3$  compositions with  $x = 0, 0.05, 0.1$  are well-known as perovskite-structure relaxor materials: by opposition to a “normal” ferroelectric which shows indeed a sharp ferroelectric–

paraelectric phase transition at a well defined temperature (called Curie temperature), they exhibit a diffuse phase transition (DPT) appearing in the weak field permittivity curve versus temperature [2]. The permittivity shows, indeed, a broad maximum over a large range of temperature which is frequency dependent. This behaviour, resulting from their nanostructure, occurs around the maximum permittivity temperature. Such nanostructures can be described as nanopolar domains distributed in a polar matrix [3].

The purpose of this paper is to study the electromechanical behaviour of  $0.9\text{PMN}-0.1\text{PT}-0.12\text{MgO}$  ceramics and to attempt to explain it with respect to the contribution of its nanostructure:

\* Corresponding author. Tel.: +33-5-55-45-2222; fax: +33-5-55-79-0998.

E-mail address: m.lejeune@ensci.fr (M. Lejeune).

1. At first, the initial nanostructure of the materials, before application of a high electric field is identified at different temperatures through weak-field permittivity measurements on a large frequency range.
2. Secondly, the sensitivity of this nanostructure to the application of a high electric field is studied through DC electric field permittivity measurements, performed at different temperatures.
3. Moreover, the nanoscale composition of the materials is determined by EDXS (energy dispersive X-ray spectroscopy) and EELS (electron energy loss spectroscopy) by TEM, in order to characterise its chemical heterogeneity and forward explain the evolution of the nanostructure with temperature and amplitude of electric field.
4. The electromechanical behaviour of 0.9PMN–0.1PT ceramics is determined according to the amplitudes of the electric field and the compressive stress applied for different temperatures. The addition of a sinusoidal electrical signal with variable amplitude and frequency to a DC electric field is finally performed at room temperature to evaluate the potentialities of 0.9PMN–0.1PT ceramics for active vibration control.

## 2. Sample preparation

(1– $x$ ) PMN– $x$  PT ceramics with  $x = 0, 0.05, 0.10$  were prepared from high-purity-grade powders of PbO, MgO, Nb<sub>2</sub>O<sub>5</sub>, TiO<sub>2</sub> according to a procedure described in earlier work [4]. A MgO excess (12 mol%) was added to the initial mixture to promote the formation of the perovskite phase and its stability during sintering and to limit consequently the presence of a pyrochlore phase (Pb<sub>2</sub>Mg<sub>0.33</sub>Nb<sub>1.66</sub>O<sub>6.52</sub>) [5]. The deficiency of every sintered sample in lead oxide was deduced from the weight loss during sintering added to the evaporated PbO content during calcination. It corresponds respectively to 4.8 and 5 mol% for 0 and 10 mol% PT. No pyrochlore phase was detected by X-ray diffraction for PMN–0.12MgO and the one identified on the surface of 0.95PMN–0.05PT and 0.9PMN–0.1PT samples was eliminated by polishing.

The theoretical densities of ceramics were determined from the relative amounts of phases and densification factors were deduced from the geometrical densities. They were around 94%.

X-ray diffraction patterns of the crushed sintered samples also revealed that free MgO was associated to the perovskite phase. It corresponds to inter or intra-granular inclusions identified by scanning electronic microscopy. The amount of free MgO was evaluated by X-ray diffraction. Thus, 6 mol% of free MgO was found in the samples. Taking into account the initial MgO

excess (12 mol%), we can conclude that 6 mol% of MgO has diffused in the perovskite structure during sintering. As the pyrochlore phase (Pb<sub>2</sub>Mg<sub>0.33</sub>Nb<sub>1.66</sub>O<sub>6.52</sub>) previously identified in the stoichiometric samples is Mg deficient compared to PMN, the stabilisation of the perovskite phase can be explained by the partial insertion of MgO in the structure.

## 3. Characterisation of the sensitivity of the PMN-PT ceramics nanostructure to the temperature and to the application of an electric field

### 3.1. Study of the evolution of the 0.9PMN–0.1PT nanostructure with decreasing temperature

At first, dielectric measurements, performed at 1 V/rms on a low frequency range (100 Hz–10 kHz) from –30 to 250°C reveal that the Curie–Weiss law is no more respected from a temperature  $T_d$  which is largely above the temperature of the maximum permittivity ( $T_m$ ), as shown in Fig. 1 for 0.9PMN–0.1PT–0.12MgO ( $T_m \approx +36^\circ\text{C}$ ).

Indeed, the temperature  $T_d$  corresponds to the appearance of a local polarisation [6–8], which can be evaluated according to Cross [9] from the following relation:

$$\left[\frac{dE}{dP}\right]_s = \alpha \cdot (T - T_0) + \alpha^2 \cdot P^2 \cdot \frac{T}{C^P}$$

Consequently, the material can be described under  $T_d$  as polar clusters distributed in a paraelectric matrix.

In a second stage, the dielectric measurements at 1 V/rms were carried out on a larger frequency range, from 100 Hz to 1 GHz for different temperatures below  $T_d$ . The real part of the permittivity, reported as a function of the frequency (Fig. 2) shows dielectric relaxation which can be attributed to a simple Debye mechanism for temperature above 60°C and to a superposition of different Debye mechanisms below 60°C.

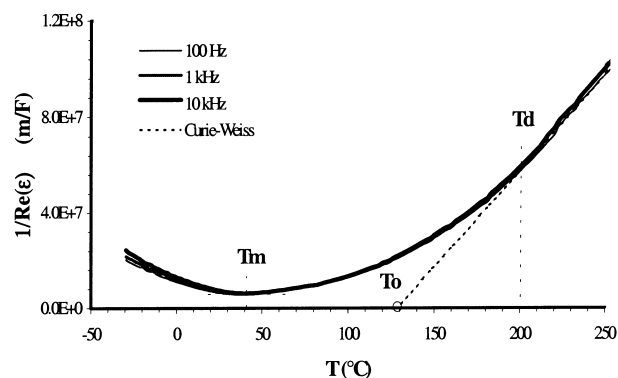


Fig. 1. The inverse of the real part of the permittivity as a function of temperature for 0.9PMN–0.1PT–0.12MgO.

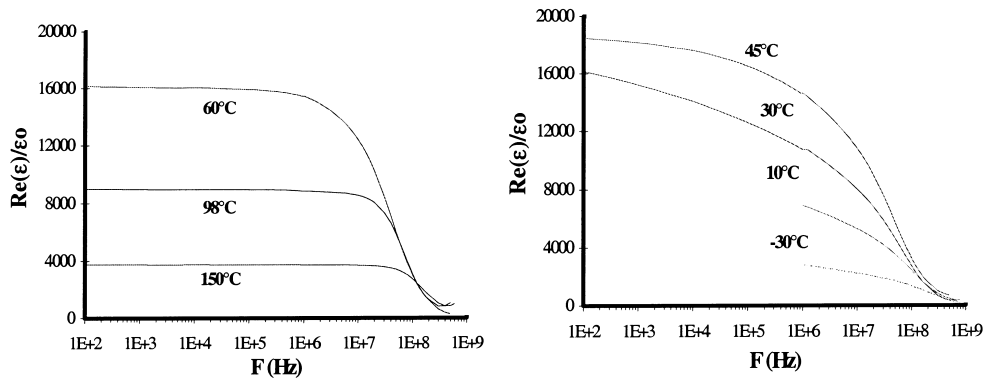


Fig. 2. Real part of the permittivity as a function of frequency at different temperatures (–30, 150°C), for 0.9PMN–0.1PT–0.12MgO.

Consequently, the imaginary part of the permittivity  $\varepsilon''$  as a function of the frequency can be decomposed at different temperatures in terms of a multi-Debye process:

$$\varepsilon''(\omega) = (\varepsilon_s - \varepsilon_\infty) \cdot \sum_i \frac{a_i \cdot \omega \cdot \tau_i}{1 + \omega^2 \cdot \tau_i^2}$$

where  $a_i$  is the weight coefficient which represents the contribution of each Debye term (Fig. 3). One can observe a relaxation time distribution which becomes larger with decreasing temperature.

This distribution can be correlated to a nucleation and growth mechanism of the polar clusters below  $T_d$ . In fact, as the stability of a polar domain increases with its size, the low relaxation times obtained at high temperature correspond to very small size polar clusters. When the temperature decreases, the broadening of the relaxation time distribution means that the size distribution of the clusters becomes larger.

### 3.2. Effect of a DC electric field (0.5 kV/mm) on the nanostructure of the materials

As previously shown by weak-field dielectric measurements on a large frequency range, 0.9PMN–0.1PT–0.12MgO ceramics can be described under  $T_d$ , as polar clusters distributed in a paraelectric matrix.

However, the electromechanical behaviour of this material is characterised under high electric field (0–2 kV/mm) to have significant responses. Therefore, we have attempted to determine the sensitivity of the material to the application of a DC electric field in order to correlate the electromechanical properties to the nanostructure of the materials. Consequently, the evolution of the nanostructure was determined through dielectric permittivity measurements, performed at 1 V/rms at the frequency range 20 Hz–20 kHz from –20 to 80°C under a 0.5 kV/mm bias.

As shown in Fig. 4, the frequency dispersion of the imaginary part of the permittivity is modified by application of a 0.5 kV/mm DC electric field, which corresponds to a variation of the distribution size of the polar domains. In fact, as observed in Fig. 5, the weight of the large size domains increases correlatively, which means that the application of a high electric field, by energy input, promotes the transition of the paraelectric matrix.

Moreover, for a constant 0.5 kV/mm DC bias, one can note (Fig. 6) that the weight of the small size polar domains ( $a_6$ ) continuously decreases with decreasing temperature. This growth mechanism is especially pronounced at a temperature  $T_i$  close to ambient. This phenomenon might be associated to the transition of the residual paraelectric matrix so that the material could

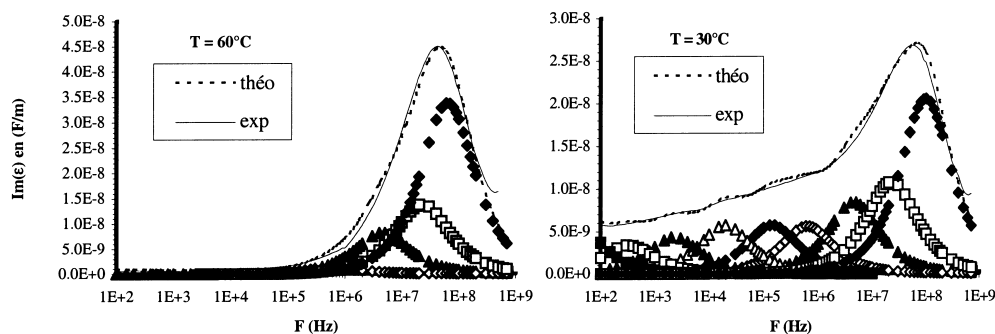


Fig. 3. Multi-Debye fitting of the imaginary part of the permittivity as a function of the frequency for 0.9PMN–0.1PT–0.12MgO at different temperatures.

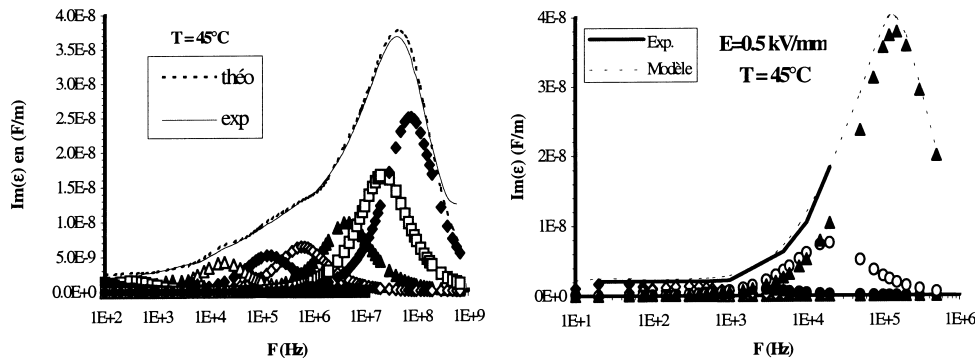


Fig. 4. Multi-Debye fitting of the imaginary part of the permittivity as a function of the frequency for 0.9PMN–0.1PT–0.12MgO at 45°C for 0 and 0.5 kV/mm DC biases.

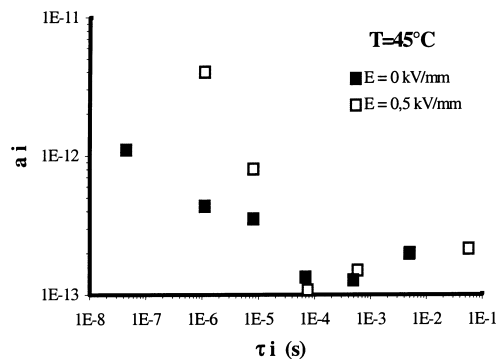


Fig. 5. Relaxation time distribution  $a_i^E(t_i)$  for 0.9PMN–0.1PT–0.12MgO at 45°C for 0 and 0.5 kV/mm DC biases.

be considered in a macroscopic ferroelectric state below this temperature [10,11]. This hypothesis will have to be confirmed by TEM observations performed in similar conditions.

#### 4. Identification of the nanoscale chemical compositions of the sintered samples

The relaxor behaviour of  $(1-x)\text{PbMg}_{1/3}\text{Nb}_{2/3}\text{O}_3-x\text{PbTiO}_3$  ceramics with  $x = 0, 0.05, 0.1$  has commonly

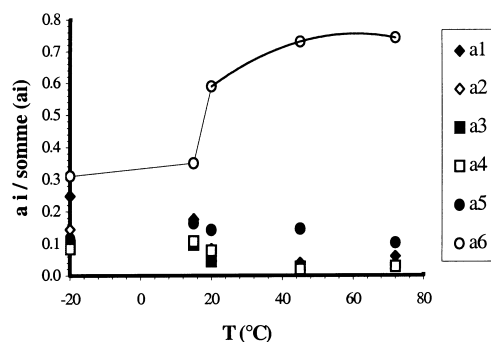


Fig. 6. Relaxation time distribution  $a_i^E(T)$  (normalised to the sum of  $a_i$ ) for 0.5 kV/mm DC bias and 0.9PMN–0.1PT–0.12MgO composition.

been explained through chemical heterogeneities [12,13]. In fact, as each chemical composition is characterised by a Curie temperature, consequently, the fluctuation of the chemical composition through the material induces a diffuse transition on a large range of temperature.

As this hypothesis has never been previously confirmed directly, nanoscale chemical analysis of PMN-PT materials were carried out by TEM through EDXS and EELS techniques. The different experimental details relative to these specific quantitative analyses have been reported in a previous paper [14]. This study has revealed large fluctuations of the local composition around the nominal one (Fig. 7): lead and magnesium deficient areas enriched in niobium coexist with nanodomains largely enriched in lead and slightly in magnesium.

The distribution of the chemical composition leads:

- to the formation of polar clusters at a temperature  $T_d(\approx 200^\circ\text{C})$ , largely above the transition temperature of the nominal composition (around  $40^\circ\text{C}$  for 0.9PMN–0.1PT–0.12MgO);
- to the nucleation and growth mechanism of polar clusters with decreasing temperature, corresponding to the transitions of the different local compositions;

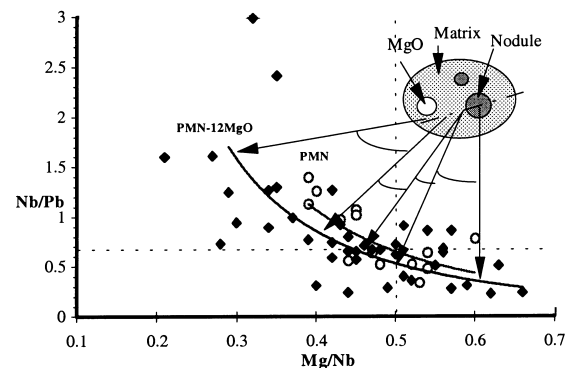


Fig. 7. Local chemical compositions identified by TEM using EDX spectroscopy (2–20 nm probe size).

- (iii) however, due to such heterogeneities, the material remains mainly paraelectric up to very low temperature but this effect can be balanced by the application of a high electric field which induces the growth of the polar clusters by displacement of their interface with the paraelectric matrix and orientation of their polarisation in the direction of the electric field which can lead to a macroscopic ferroelectric transition in specific conditions of temperature and electric field intensity.

## 5. Electromechanical behaviour of 0.9PMN–0.1PT ceramics

### 5.1. Electromechanical behaviour of 0.9PMN–0.1PT ceramics under quasi-static electric fields and variable compressive stress

Strains induced by the application of variable electric field (0–1 kV/mm) and uniaxial stress (5–100 MPa) were determined in 0.9PMN–0.1PT–0.12MgO at different temperatures from 8–45°C.

They correspond to the sum of the two following contributions:

- the strain of the material as a function of the stress without electric field, evaluated by the determination of the Young modulus by ultrasounds propagation techniques [15,16];
- the field-induced strain for variable uniaxial stress. So, 20 mHz field induced longitudinal strains were measured using a linear variable differential transformer for different uniaxial stress controlled by a pressure gauge.

In this way, the total strain  $x_T^X(E)$  induced by simultaneous application of electric field ( $E$ ) and uniaxial

stress ( $X$ ) has been calculated for 0.9PMN–0.1PT for the different temperatures and it is reported in Fig. 8 at room temperature i.e.  $x_{21^\circ\text{C}}^X(E)$ . The characteristics obtained at 8°C i.e.  $x_{8^\circ\text{C}}^X(E)$  exhibit a faster saturation and larger hysteresis. In fact, the hysteresis of the field-induced strain results from the displacement of the interface between polar and paraelectric phases which induces a dissipation of energy due to some defects in the material. According to the previous results, it was shown that the polar volume rapidly increases below 20°C for 0.9PMN–0.1PT when a 0.5 kV/mm electric field is applied (Fig. 6).

Therefore, the fast saturation and large hysteresis of the field-induced strains below 20°C are in good agreement with this phenomenon.

The characteristics  $x_T^E(X)$  can be deduced from the curves  $x_T^X(E)$ , obtained for  $T = 45, 21$  and  $8^\circ\text{C}$ , respectively, by reporting the average value of the longitudinal strains corresponding to different magnitude of the electric field, as a function of the stress (Fig. 9).

It appears that 0.9PMN–0.1PT ceramics exhibit a more pronounced complex macroscopic non linear electromechanical behaviour when the electric field is high or the temperature is low; consequently, the experimental  $x_T^E(X)$  curves can be fitted as polynomial functions of  $E$  and  $X$ :

$$x_T(X, E) = \sum_i \left( \sum_j M_{ij}^T * E^j \right) * X^i$$

with  $i = 0 \dots 2$  and  $j = 0 \dots 3$

for  $X$  and  $E$  ranging respectively from 0–40 MPa and from 0–0.5 kV/mm, with  $M_{ij}$  a function of the temperature, which reveals a strong dependence of the apparent elastic compliance with the electric field and stress, according to the range of temperature.

In fact, the apparent elastic compliance  $s$  (1/Pa), defined by the following relation:

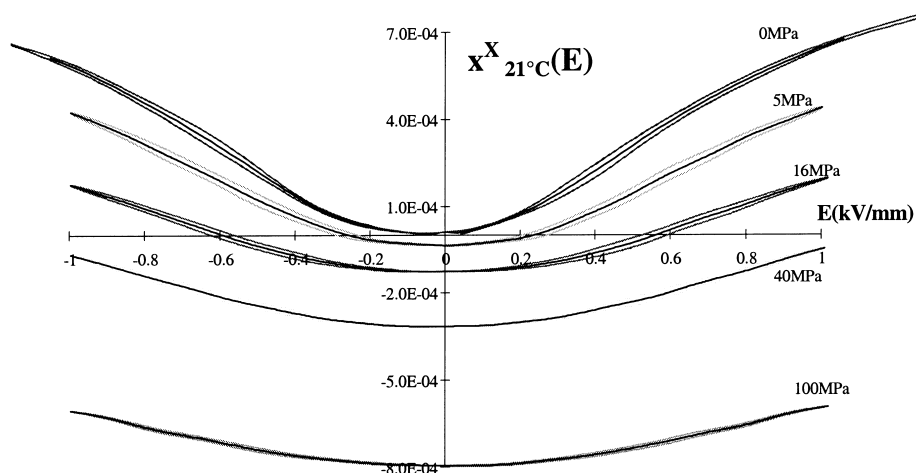


Fig. 8. 0.9PMN–0.1PT total strain induced by simultaneous application of electric field ( $E$ ) and uniaxial stress ( $X$ ) at room temperature:  $x_{21^\circ\text{C}}^X(E)$ .

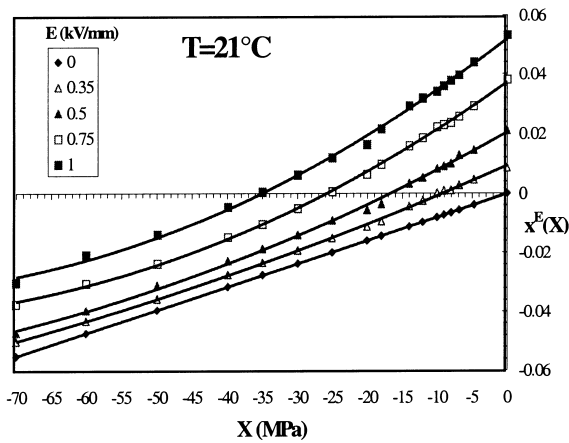


Fig. 9. 0.9PMN–0.1PT electromechanical strain  $x_{21}^E(X)$ .

$$s_T^{E_0}(x) = \left. \frac{\partial x(E, X)}{\partial X} \right|_{E_0}$$

can be deduced from the functions  $x_T(E, X)$  previously determined at different temperatures respectively 8, 21 and 45°C and correspond to polynomial functions of  $E$  and  $X$  such as

$$s_T(X, E) = \sum_i \left( \sum_j A_{ij}^T * E^j \right) * X^i$$

with  $i = 0 \dots 2$  and  $j = 0 \dots 3$

for  $X$  and  $E$  ranging respectively from 0–40 MPa and from 0–0.5 kV/mm, with  $A_{ij}$  a function of the temperature.

The surfaces  $s_T(X, E)$  are presented in Fig. 10: the dependence of 0.9PMN–0.1PT–0.12MgO elastic compliance with the electric field, temperature and stress can be correlated to the evolution of its nanostructure with these different parameters. In fact, as previously shown, the polar volume increases with decreasing temperature or increasing electric field; therefore, as this phenomenon is associated to an increase of the elastic compliance, one can conclude that the polar phase exhibits a higher compliance than the paraelectric matrix.

Otherwise, the application of an increasing stress stiffens the material once it is polarised under a 0.5 kV/mm electric field (Fig. 10). Taking into account the higher elastic compliance of the polar clusters compared to the paraelectric phase, this shows that the development of the polar volume induced by the electric field can be balanced by the application of a stress.

Consequently, 0.9PMN–0.1PT ceramics are characterised by a tunable compliance: they are capable of adjusting their response to a stress (i.e. their strain) by the variation of the applied electric field. Therefore, these materials seem very attractive for active damping applications for which the vibrations of the systems  $[\delta x(t)]$  i.e.  $\delta X(t)$  are cancelled by application of an appropriate feedback electric field  $[\delta E(t)]$ . For such devices, the ceramic has a double function of sensor and actuator which must be characterised (i) as a sensor, by the sensitivity of the polarisation with the stress according to the applied electric field (ii) as an actuator, by the variation of the strain with the applied electric field for different compressive stresses. The part (ii) has been performed at room temperature by adding a sinusoidal electrical signal to a DC electric field set to 0.6 kV/mm, because this corresponds to the maximum sensitivity  $(\delta x / \delta E)$  according to previous results (Fig. 8).

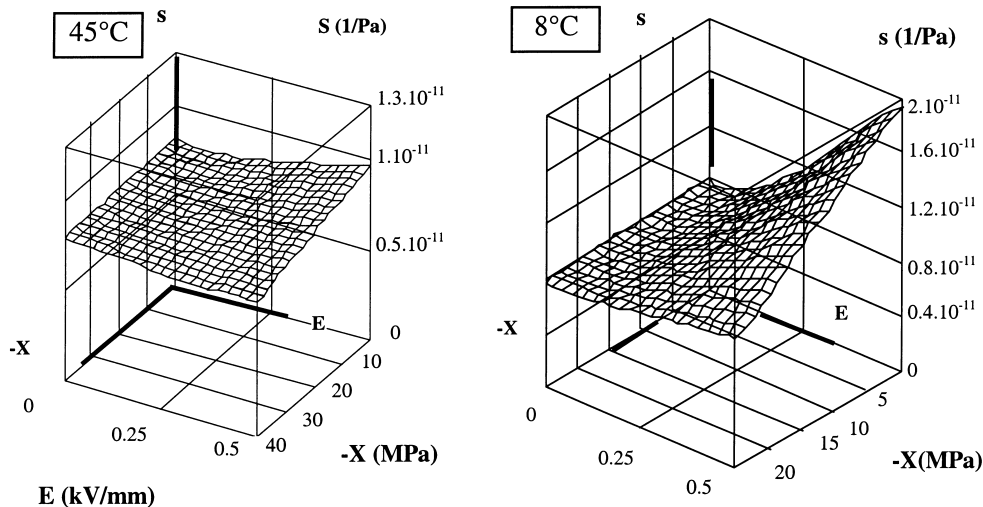


Fig. 10. Surface curves corresponding to the dependence of 0.9PMN–0.1PT elastic compliance ( $s$ ) with the amplitudes of electric field ( $E$ ) and the stress ( $X$ ) at 8 and 45°C.

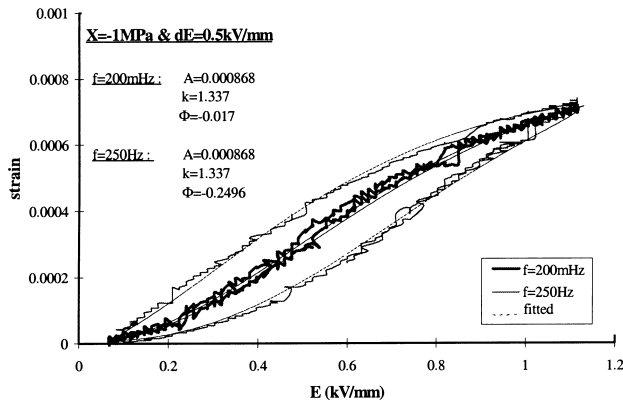


Fig. 11. 0.9PMN–0.1PT room temperature strain induced by application of a sinusoidal signal of 0.5 kV/mm amplitude and variable frequency (200 mHz or 250 Hz) added to a 0.6 kV/mm DC electric field for a 1 MPa compressive stress.

### 5.2. Electromechanical behaviour of 0.9PMN–0.1PT ceramics under dynamic electric fields and variable compressive stress

The electromechanical response as actuator has been measured, at room temperature for different compressive stresses ranging from 0 to 30 MPa, by applying a sinusoidal signal of variable amplitude (from 0.1–0.5 kV/mm) and frequency (20 mHz–1 kHz) in addition to a 0.6 kV/mm DC electric field.

As shown in Fig. 11, the increase of the frequency from 200 mHz to 250 Hz for a given amplitude of the sinusoidal signal (0.5 kV/mm) and of the compressive stress (1 MPa) leads to the enhancement of the hysteresis. So, these characteristics cannot be analysed by the way used previously in part 5.1 at low frequency, which consists in taking the average value of the strain for different magnitude of the electric field. (Note that this method which consequently neglects the hysteresis of the field-induced curves becomes also partly invalid for the treatment of the quasi-static field-induced strain at 8°C because of the corresponding hysteresis at this temperature.)

The electromechanical behaviour observed in Fig. 11 is very well described in terms of a hyperbolic tangent squared formulation which moreover allows to take into account the hysteresis of the curves through the addition of a phase delay ( $\phi$ ) i.e.:

$$x = A \tan^2[k(E_0 + dE \sin(\omega t + \phi))]$$

where the parameters  $A$  and  $k$  only depend on applied compressive stress as shown in Figs. 11–13 while  $\phi$  is function of pulsation ( $\omega$ ) of the sinusoidal electric field.

Moreover, to validate the potentialities of 0.9PMN–0.1PT ceramics for active vibration control, the determination of the polarisation as a function of the stress is in progress, in order to know its behaviour as a pressure sensor capable of detecting a vibration.

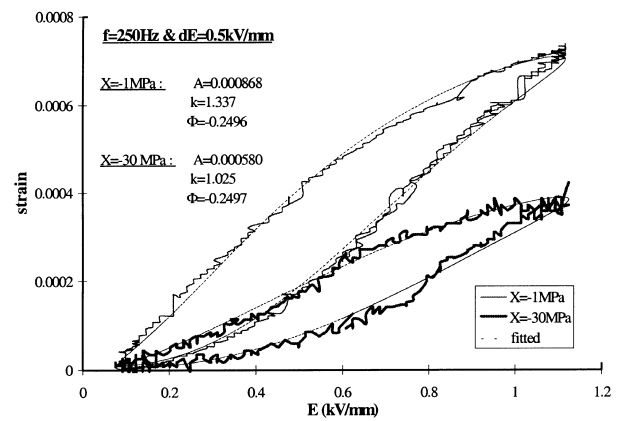


Fig. 12. 0.9PMN–0.1PT room temperature strain induced by application of a 250 Hz sinusoidal signal of 0.5 kV/mm amplitude added to a 0.6 kV/mm DC electric field for compressive stress of 1 or 30 MPa.

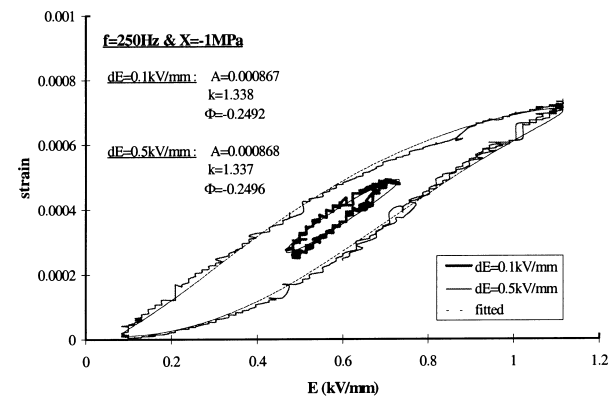


Fig. 13. 0.9PMN–0.1PT room temperature strain induced by application of a 250 Hz sinusoidal signal of variable amplitude (0.1 or 0.5 kV/mm) added to a 0.6 kV/mm DC electric field for a 1 MPa compressive stress.

## 6. Conclusions

This study has shown a strong dependence of 0.9PMN–0.1PT apparent elastic compliance with the temperature, the electric field and the stress. This behaviour is attributed to the growth of compliant polar clusters induced by decreasing temperature or increasing electric field and inhibited by the application of an uniaxial stress. Therefore, this material can be considered as a smart material, able to adjust its response (i.e. its strain) by the variation of one of these three parameters. It seems very attractive in particular for active damping applications.

## Acknowledgements

The authors wish to thank the DGA for their financial support of this study.

## References

- [1] K. Uchino, *Am. Ceram. Soc. Bull.* 65 (4) (1986) 647.
- [2] G.A. Smolenski, *J. Tech. Phys. USSR* 28 (1958) 7.
- [3] G. Burns, F.H. Dacol, *Ferroelectrics* 109 (1990) 5.
- [4] E. Lattard, M. Lejeune, P. Abelard, *J. Phys. III* 4 (1994) 1165.
- [5] O. Bouquin, M. Lejeune, J.P. Boilot, *J. Am. Ceram. Soc.* 74 (5) (1991) 1152.
- [6] G. Burns, F.H. Dacol, *Ferroelectrics* 104 (1990) 25.
- [7] E. Husson, N. Mathan, G. Calvarin, J.R. Gavarri, A.W. Hewat, A. Morell, *J. Phys. Condens. Matt* 3 (1991) 8159.
- [8] E. Husson, P. Bonneau, G. Calvarin, J.R. Gavarri, A.W. Hewat, A. Morell, *J. Solid State. Chemistry* 91 (1991) 350.
- [9] L.E. Cross, *Ferroelectrics* 76 (1987) 241.
- [10] E. Husson, M. Malki, M. Chabin, A. Morell, *Journal de Physique III* 4 (1994) 1151.
- [11] S.J. Butcher, M. Daglish, *Ferroelectrics Letter* 10 (1989) 117.
- [12] V.A. Isupov, *Soviet Physics, Technicals Physics* 1 (1956) 1846.
- [13] G.A. Smolenski, *J. of the Physical Society of Japan* 28 (1970) 26–37.
- [14] E. Lattard, M. Lejeune, R. Guinebretière, D. Imhoff, P. Abelard, *J. Phys. III* 7 (1997) 1173.
- [15] P. Fleury, J.P. Mathieu, *Vibrations Mécaniques Acoustiques*, Eyrolles, Paris, 1955.
- [16] R.T. Beyer, S.V. Letcher, *Physical Ultrasonics*, Academic Press, New York and London, 1969.